

Experimental research on seismic behavior of a composite RCS frame

Jinjie Men^{*}, Yarong Zhang^a, Zhifeng Guo^b and Qingxuan Shi^c

*College of Civil Engineering, Xi'an University of Architecture & Technology,
13 Yanta Road, Xi'an, Shaanxi Province, 710055, China*

(Received June 11, 2014, Revised October 07, 2014, Accepted October 10, 2014)

Abstract. To promote greater acceptance and use of composite RCS systems, a two-bay two-story frame specimen with improved composite RCS joint details was tested in the laboratory under reversed cyclic loading. The test revealed superior seismic performance with stable load versus story drift response and excellent deformation capacity for an inter-story drift ratio up to 1/25. It was found that the failure process of the frame meets the strong-column weak-beam criterion. Furthermore, cracking inter-story drift ratio and ultimate inter-story drift ratio both satisfy the limitation prescribed by the design code. Additionally, inter-story drift ratios at yielding and peak load stage provide reference data for Performance-Based Seismic Design (PBSD) approaches for composite RCS frames. An advantage over conventional reinforced concrete and steel moment frame systems is that the displacement ductility coefficient of the RCS frame system is much larger. To conclude, the test results prove that composite RCS frame systems perform satisfactorily under simulated earthquake action, which further validates the reliability of this innovative system. Based on the test result, some suggestions are presented for the design of composite RCS frame systems.

Keywords: composite structure; RCS; composite joint; capacity; ductility; seismic response

1. Introduction

Composite RCS moment frame systems typically consist of Reinforced Concrete (RC) columns and structural Steel beams (RCS). Using RC rather than structural steel columns can result in significant material cost savings, increased inherent structural damping, and significantly increased lateral stiffness of the building (Griffis 1986, Michael *et al.* 2000, Liang and Parra-Montesinos 2004). Many kinds of details on composite RCS joints were proposed in the US, Japan and China (Sheikh *et al.* 1989, Parra-Montesinos and Weight 2000, Chou and Wu 2007), and many experimental studies have been conducted to make sure of seismic performance of the joint (Fargier-Gabaldón and Parra-Montesinos 2006, Chou *et al.* 2008, Guo *et al.* 2012, Bahman *et al.* 2013). In 1994, ASCE published design guidelines for composite RCS joints in low to moderate

*Corresponding author, Professor, E-mail: men2009@163.com

^a Master Student, E-mail: 1027326257@qq.com

^b Ph.D. Student, E-mail: guozhifeng2007@126.com

^c Professor, E-mail: shi_qx@126.com

seismic regions (ASCE 1994).

However, to establish a rational design method of RCS composite structure, it is necessary to clarify the overall frame behavior. So far, only a few tests of the composite RCS frame are reported. A two-bay, two-story frame specimen was tested under reversed cyclic loading by Nozomu and Yasushi (2000) to study the effect of joint failure on the overall frame behavior. Pseudo-dynamic test of a full-scale three-story three-bay composite steel concrete frame was conducted by Chen *et al.* (2004) and Cordova *et al.* (2004) to study the response and damage patterns of the RCS frame under the earthquake loading events. A series of cyclic tests of a full-scale one-story two-bay post-tensioned RCS frame were conducted by Chou and Chen (2010) to examine the connection performance, progress of damage and strength degradation of the frame. The above tests show the RCS frame behaviors stably and performs very well under earthquake ground motions. However studies are still very few to reveal the seismic behavior and characteristics of RCS composite frame. With the goal to facilitate greater acceptance and use of RCS system for seismic design, a two-bay, two-story moment frame, with an improved RCS joint detail, was design and tested under cyclic loading in this research to: (1) assess and demonstrate the seismic performance of RCS frame; (2) provide data and interpret information that support the development of Performance-Based Seismic Design (PBSD); and (3) develop seismic design provisions for composite RCS frames. The experimental program and the test result are presented and discussed here in this paper.

2. Composite RCS joint

From the point of seismic design, a significant advantage of RCS systems lies in the design and performance of the joint details. Shown in Fig. 1(a) is the typical composite RCS joint designed and used in the research. The main component of the beam and column are both continuous. The steel beam web passes continuous through the joint, thereby avoiding interruption of the beam entirely at the column face. The steel beam flanges extend into the joint and are partly cut off, which can keep the longitudinal reinforcement of the column passing through the joint and facilitate casting and vibrating the concrete. Other joint details, such as extend face bearing plates, steel band plates, cover plate and X shape reinforcement bar can be welded on the typical RCS

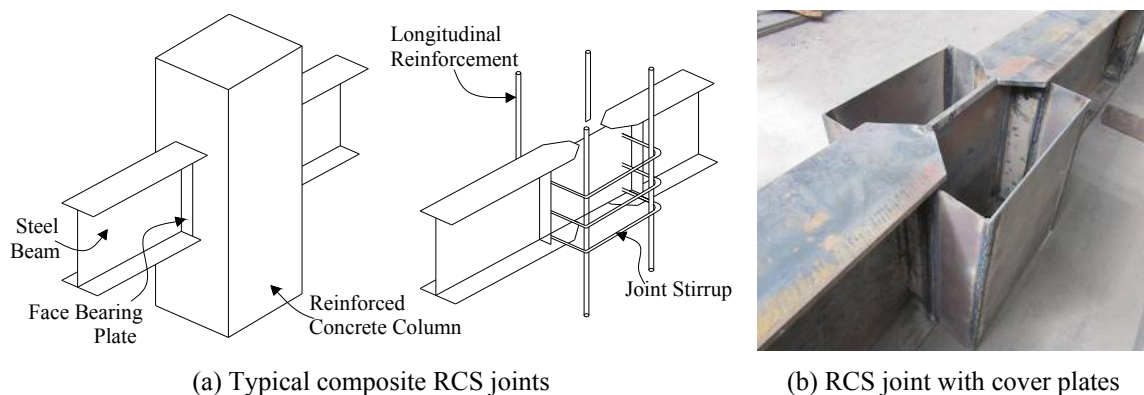


Fig. 1 Composite RCS joints

joint. According to the numerical simulation result described by Men *et al.* (2012), RCS joint with cover plate, shown in Fig. 1(b) takes on excellent strength and deformation capacity. Hence it is used to construct the RCS frame which will be introduced in the next section.

3. Experimental program

3.1 Description of the specimen

The two-bay two-story frame has a scale of 1/3 to the prototype frame. The span of each bay is 2000mm and the height of each story is 1200 mm. The square cross section of the reinforced concrete columns is 200 mm × 200 mm and the H section of the steel beam is 100 mm × 68 mm × 4.5 mm × 7.6 mm. Column longitudinal reinforcement included four 16 mm deformed bars, representing approximately 2.0% of the column gross area. The dimension and the details of the specimen are shown in Fig. 2.

The construction and loading of this test frame was carried out in Key Laboratory of Structural Engineering and Seismic Resistance, Ministry of Education, China. Before casting the concrete, the longitudinal reinforcement and stirrup of the foundation are assembled. Then the longitudinal reinforcement of the column was fixed into the foundation. Next the column stirrups and the steel beam of 1st story were assembled. And then the column stirrups and the steel beam of 2nd story were assembled by the same way. Figs. 3(a)-(d) show the assembly of the beam-column connection for the exterior and interior joint, the assembly of the overall frame and the frame when applying load in the laboratory, respectively.

3.2 Material properties

Grade HRB335 deformed steel bars were used for all the reinforcement in the foundation and columns. And Grade Q235 steel was used for all the steel beam, FBPs and other steel plates. The

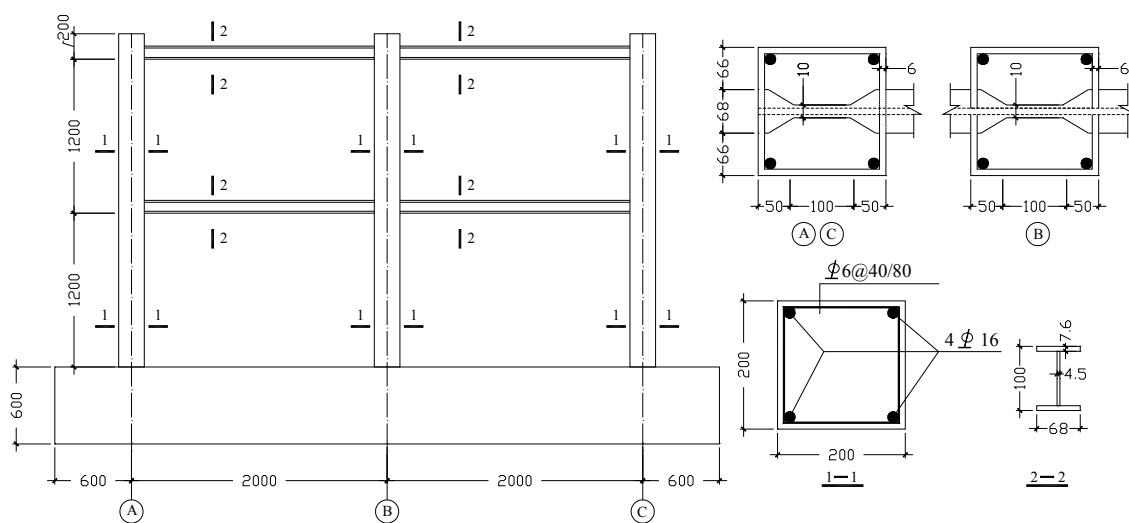


Fig. 2 Dimension and steel reinforcement details of the specimen

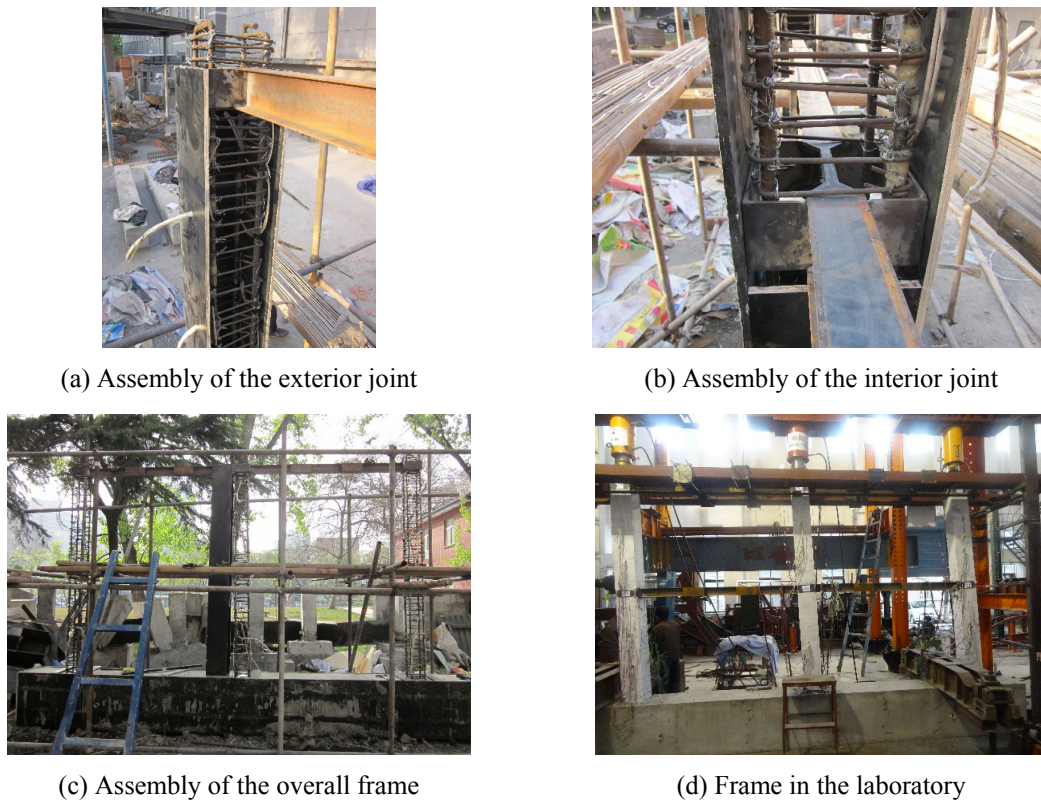


Fig. 3 Composite RCS frame

Table 1 Material properties

Items	Depth or diameter/mm	f_y / MPa	f_u / MPa	E_s / 10^5 MPa	ϵ_y / $\mu\epsilon$
Flange and web	-	359.9	515.7	2.04	1764
Cover plates	6	243.0	379.0	1.97	1234
Rebars	16	350.0	535.0	1.89	1852
	6	320.0	445.0	1.97	1624

Note: $\mu\epsilon = \Delta L / L \times 10^{-6}$

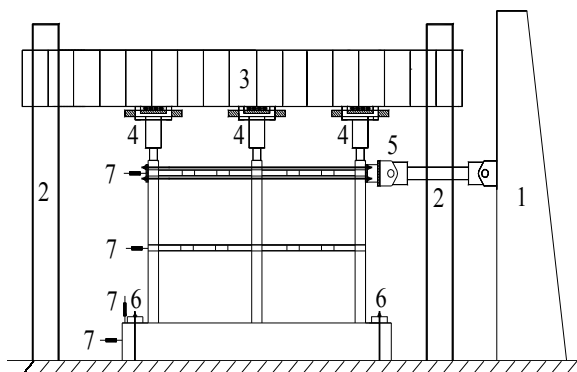
material properties of the reinforcement and the steel were obtained based on three coupons for each reinforcement bar or steel plate. And the strengths of the reinforcement and the steel, also with the elastic modulus and yielding strain, are listed in Table 1. The concrete design strength grade is C60. And the concrete compressive strengths for foundation and columns at test day are 58.8Mpa and 57 Mpa, which also were obtained based on three cubes for each concrete pour.

3.3 Test setup, load and displacement history and instruments

The test setup used for the experimental program is shown in Fig. 4. Axial compression load was applied to the columns through three hydraulic jacks, which is determined by the design axial

compression ratio of 0.15 and 0.3 for the side column and middle column, respectively. Then lateral reversed-cyclic displacements were applied at the top of the column through a 500 kN hydraulic actuator. The load and displacement history includes two stage: elastic cycle and inelastic cycle. Before yielding, load cycles were applied to the specimen, which increased by 10 kN in each elastic cycle. After yielding, displacement cycles were applied to the specimens, with displacement increases by Δ_y (a scale of the yielding displacement). Each displacement cycle was repeated twice to study the stiffness and strength deterioration at that drift level. When the lateral load reduced to about 85% of the peak load, the test was stopped. The load and displacement history is shown in Fig. 5.

A load cell and two displacement transducer were used to monitor the applied lateral load and displacement on the 1st and the 2nd floor, respectively. A displacement transducer was also placed near the bottom of the RC column to monitor slip in the test setup, which was subtracted from the applied lateral displacement to determine the actual drift. The story drift levels in the experimental results presented in this paper refer to the actual drift levels experienced by the specimens. Linear



1. reaction wall; 2. rigid frame; 3. rigid beam; 4. hydraulic jack; 5. hydraulic actuator; 6. bolts; 7. displacement transducer

Fig. 4 Experiment equipments

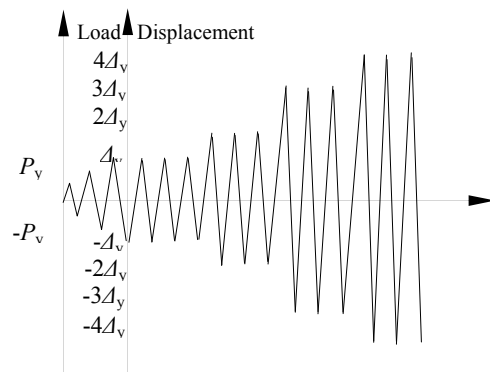


Fig. 5 Loading and displacement history

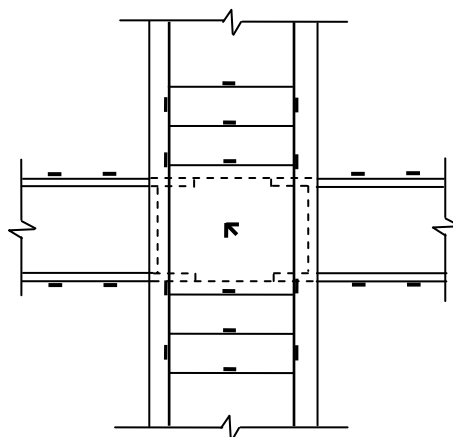


Fig. 6 Layout of strain gauges around the joint

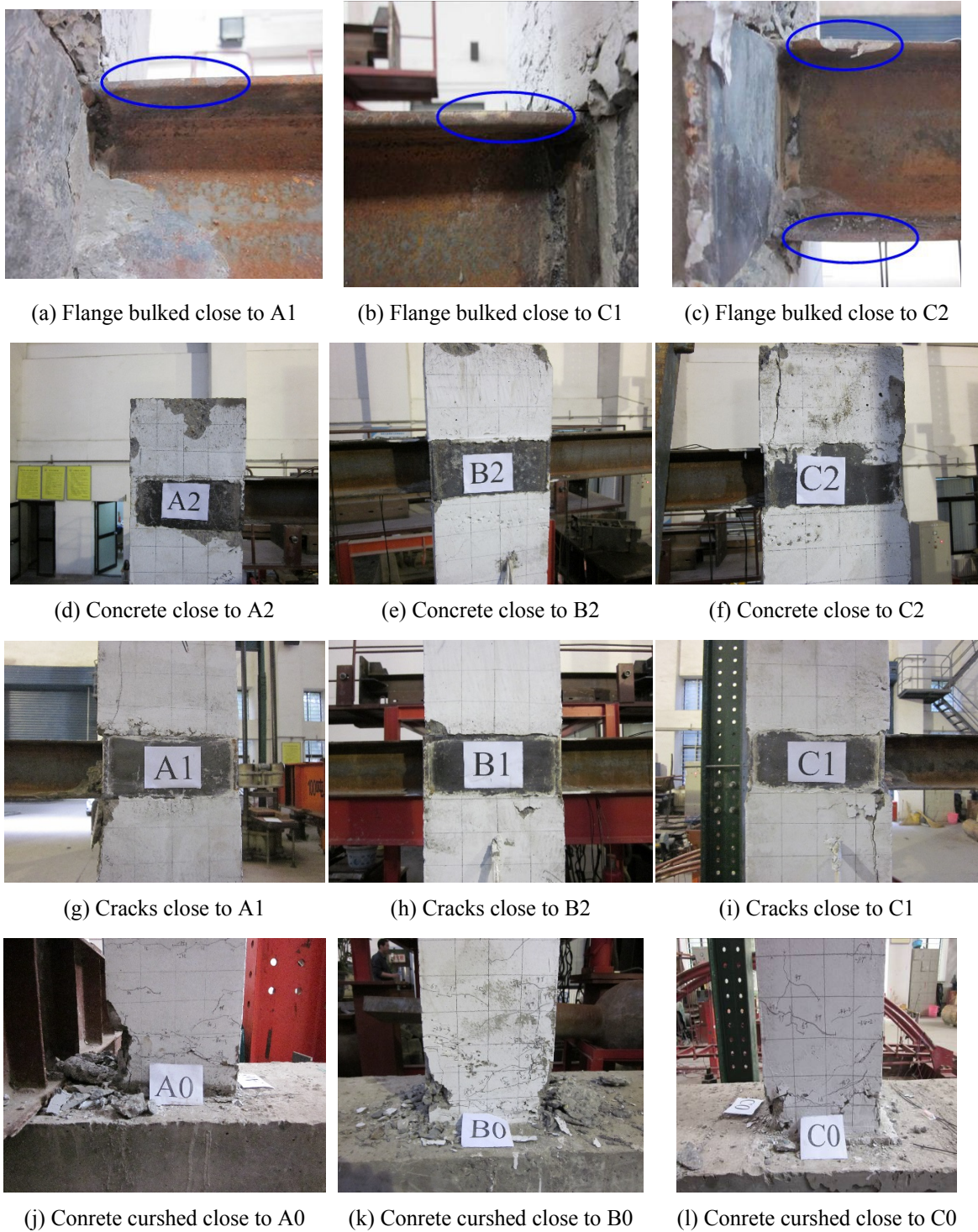


Fig. 7 Cracks of the column concrete and local buckling of the beam flange (A, B, C represent the axis number in Fig. 2 and the number following A, B, C represent the floor number)

potentiometers and clinometers were used to measure joint deformations and beam rotations. Strains in the steel beam web and flanges, and in the column reinforcement, shown in Fig. 6, were monitored through linear and rosette strain gauges.

4. Test frame results

4.1 Cracking pattern and steel beam yielding

Four key strain values were monitored to evaluate the behavior of the frame during the experiment process. They are the strain of the column longitudinal reinforcement and stirrup, the steel beam flange and web. When the lateral load reached to approximately 40 kN, the first flexural crack occurred at about 20 cm to the bottom of the exterior column. The length of the crack is about 10 mm and increased to 16 mm when the lateral load reached to -40 kN. At that time the four key strain value is $400 \mu\epsilon$, $201 \mu\epsilon$, $551 \mu\epsilon$ and $184 \mu\epsilon$, respectively. When the lateral load was applied to 50 kN, another flexural crack occurred at about 80 mm to the bottom of the exterior column and two cracks occurred at about 10 cm and 20 cm to the bottom of the interior column. All these cracks developed and accompanied with some new cracking in the column ends of the 1st and the 2nd floor when the load varied from 60 kN to -60 kN. At that time the four key strain value is $1,248 \mu\epsilon$, $415 \mu\epsilon$, $1,088 \mu\epsilon$ and $356 \mu\epsilon$, respectively. Then the displacement cycle was applied for the strain of beam flange is close to its yielding strain. At the first displacement cycle, the beam flange close to the exterior columns in the 1st and the 2nd floor became into yielding. The maximum strain of the beam flange reached to $2,066 \mu\epsilon$ and the others were all less than their yielding strain. At the second and third displacement cycle, cracks were also observed at about 80 cm to the column bottom. Then all the cracks developed and part cover concrete peeled off at the two ends of columns at the fourth and fifth displacement cycle. At the sixth displacement cycle, the beam flange in the 2nd story are local buckled and the concrete in the bottom of the interior column in 1st story were crushed out. The ultimate strength reached to about 85% of the peak strength at the eighth displacement cycle.

At the end of the test, the local buckling of the steel beam flange, marked with oval lines are shown in Figs. 7(a)-(c). And the concrete mainly crushed at the bottom of the column connected to the foundation, shown in Figs. 7(j)-(l); Cracks, shown in Figs. 7(g)-(i) also can be seen on the surface of concrete columns above or below the beam in the 1st floor; While in the 2nd floor, almost no crack can be seen on the surface of concrete columns close to the joint, shown in Figs. 7(d)-(f).

The distribution and the sequence of the plastic hinge in the frame are illustrated in Fig. 8. It is shown that whether under the load in the forward or the reverse direction, the plastic hinge first formed in one end of the steel beam. The three hinges marked with 1, 2 and 3 occurred almost the same time at the first displacement cycle. Then the other hinges occurred in the end of the beam in the other span and/or in the end of the beam in the 2nd story. And then the plastic hinge also occurred in the end of the RC columns. At the end of the test, plastic hinges occurred in every beam end and column bottom of the frame specimen. It is concluded that the composite RCS frame meet the strong-column weak-beam criterion and it is a ductile moment frame.

4.2 Strength and deformation capacity

Experimental results on the strength and the displacement are shown in Table 2. P_{cr} , P_y , P_{max}

even larger than 6. It is much larger than the requirement usually for an earthquake resistance structure.

4.3 Load versus story drift response

Load versus story drift response for the 1st floor, 2nd floor and the load versus overall displacement of the RCS frame is shown in Figs. 9(a)-(c), respectively, with the total drift corrected to account for deformations in the test setup. It can be seen that all the three hysteresis loops are plump with a bow shape, and symmetrical in the two loading directions with a little exception for the 2nd floor at the last displacement cycle due to the local buckling of the steel beam. There is almost no residual deformation at early loading cycle although cracking of the concrete were observed at the end of the columns. At larger displacement cycles, during which yielding of the steel flange or concrete crushing occurred, full hysteresis loops were still observed that led to excellent energy dissipation capacity. The RCS frame reached its maximum strength at the fifth displacement cycle with the top displacement about -63.98 mm in the reverse loading. Beyond this point, slow strength degradation was observed and the ultimate displacement of the overall frame is about -98.57 mm.

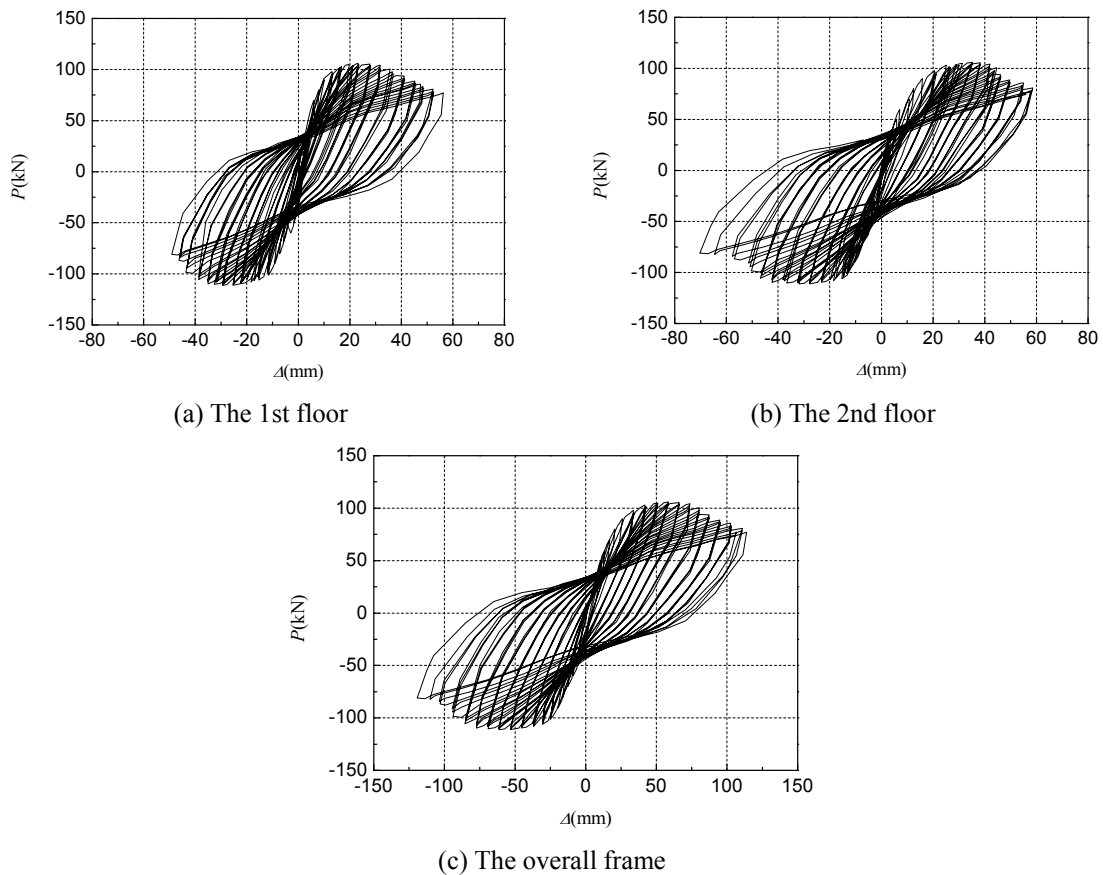


Fig. 9 Hysteretic curves of the specimen

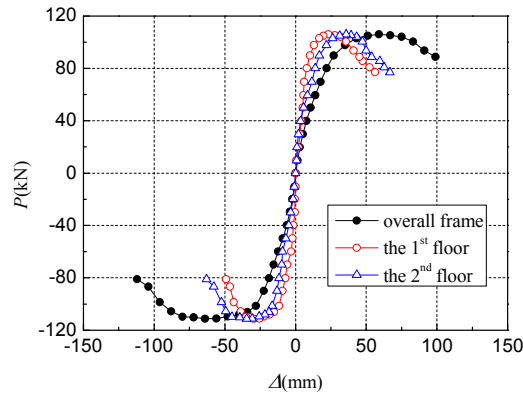


Fig. 10 Skeleton curves of the specimen

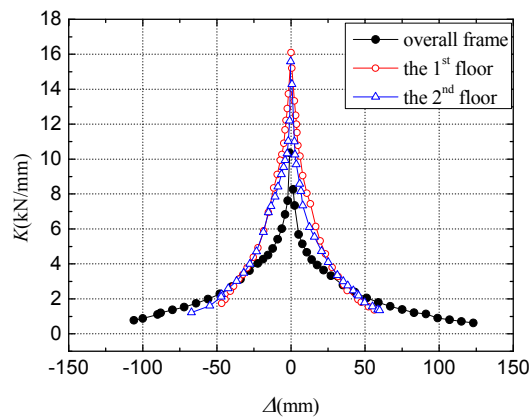


Fig. 11 Stiffness degradation of the specimen

4.4 Skeleton curves

The skeleton curves of the 1st floor, 2nd floor and the overall frame were obtained by connecting the peak points at each loading increment of the hysteretic curves, as shown in Fig. 8. From the skeleton curves, the cracking, the yielding, the maximum as well as the ultimate loading point can be easily recognized, which divide the loading process into the elastic, the elastic-plastic and the failure phases. It can be found that all the three skeleton curves are smooth especially in the forward load direction which indicates that there is no sudden failure occurred in the members of the RCS frame. Fig. 10 also shows that the initial stiffness of the two stories is similar due to the same member dimension. The deformation of the 2nd floor is a little larger than that of the 1st floor in the elastic-plastic and the failure stages. This is because that strains in the steel beam of the 2nd floor developed faster than that of the 1st floor.

4.5 Stiffness degradation

The stiffness degradation herein refers to the decrease of secant stiffness of the frame with the increasing repeated cycles and displacement. The secant stiffness of the 1st floor, the 2nd floor and

Table 3 Energy dissipation coefficient and equivalent damping coefficient

Items	E_d	h_e
Overall frame	0.83	0.133
1st floor	0.84	0.134
2nd floor	0.79	0.126

the overall frame are plotted in Fig. 11. It is shown that the three curves have the similar tendency. Especially for the 1st and the 2nd floor, they are almost the same. This indicates that the damage of the columns and beams in the two stories, which result in the decrease of the stiffness, are in the similar magnitude. In the early stage, the stiffness decreases sharply, and then the slope becomes slow in the later stage. The stiffness of the overall frame decrease faster than that of the two floors just before about $4\Delta_y$ displacement cycle ($\Delta = 38$ mm). And then it decreases lower. This is coincide with the calculated result of the overall frame stiffness, which is determined by equation K_1K_2/K_1+K_2 where K_1 and K_2 represents the stiffness of the 1st and the 2nd floor, respectively. At $4\Delta_y$ displacement cycle, the equation calculated by the two story stiffness is closed to 1, which is the boundary point influencing the slope of the stiffness degradation. When cracks appear, the stiffness reduces to less than 65% of its initial value. And the ultimate stiffness, when the strength reduced to 85% of the peak strength, is about 10% of the initial value.

4.6 Energy dissipation capacity

The energy dissipation in each loading cycle is the difference between the absorbed energy and the released energy under unloading. Energy dissipation coefficient (E_d), which can be calculated by the sum of the areas enclosed by the hysteresis loop divided by the sum of the areas of the corresponding triangle at each loading cycle, and equivalent viscous damping coefficient (h_e), which can be calculated by the energy dissipation coefficient divided by 2π , are two important indicators to evaluate the seismic performance of a structure. The two coefficients of the 1st floor, the 2nd floor and the overall frame at the peak loading cycle are listed in Table 3. It can be seen that the two coefficients of are almost the same for the story and the overall frame, only that of the 2nd floor is a little small. This indicates that the energy dissipation capacity of the RCS frame is well-proportioned. And this is helpful for preventing the frame from collapse suddenly. The equivalent damping coefficient is larger than that of a similar Steel Reinforced Concrete (SRC) frame described by Wijesundara *et al.* (2011), which also indicates that the RCS fame has a good energy dissipation capacity.

5. Conclusions

The composite RCS joint in the frame was designed to let the main component of the beam and column both pass through it continuously. The two-bay, two-story composite RCS frame specimen was tested under reversed cyclic loading and showed good seismic performance with stable load versus story drift response and excellent deformation capacity. Though the initial flexural crack appeared in the column, the plastic hinge first occurred in the end of the steel beam. The failure process of the frame meet the strong-column weak-beam criterion. The cracking and ultimate

inter-story drift ratios satisfy the corresponding limitation value well and the yielding and peak inter-story drift ratios provide reference data for the PBSO for the RCS frame. The displacement ductility coefficient of the frame is much larger than that of RC and steel moment frame. The stiffness retention and energy dissipation capacity was good till the inter-story drift ratio of approximately 1/25. The composite RCS frame test described herein further validates the reliability of this innovative system.

- (1) Composite moment frame using reinforced concrete columns and steel beams could be used as earthquake resistant structures, even in zones of high seismicity, for their excellent strength, deformation capacity and energy dissipation capacity.
- (2) When the composite RCS frame subjected to rare earthquake, concrete of the column above and below the steel beam is likely to be crushed. Hence, some details could be added in the column. For example, several layer of ties could be provided above and below the beam. In addition, vertical rods, steel angles, or other elements could be attached directly to the steel beam to transfer vertical forces into the concrete column.
- (3) The average value of cracking inter-story drift ratio, yielding inter-story drift ratio, peak inter-story drift ratio and the ultimate inter-story drift ratio, which are 1/346, 1/155, 1/39 and 1/25, could be used as the performance index for the fully operational level under frequent earthquakes, temporarily operational level under occasional earthquakes, reparably operational level under rare earthquakes and collapse prevention level under very rare earthquakes, respectively.

Acknowledgments

The research described in this paper was financially supported by the National Natural Science Foundation of China (51008244) and Natural Science Basic Research Plan in Shaanxi Province of China (2014JQ7245, 2014KJXX-67). The authors are grateful for their support. They also thank Dr. T. Schumacher of University of Delaware for his suggestion and feedback in the English writing.

References

- ASCE Task Committee on Design Criteria for Composite Structures in Steel and Concrete (1994), Guidelines for design of joints between steel beams and reinforced concrete columns, *J. Struct. Eng.*, **ASCE**, **120**(8), 2330-2357.
- Bahman, F.A., Hosein, G. and Nima, T. (2013), "Seismic performance of composite RCS special moment frames", *KSCE J. Civil Eng.*, **17**(2), 450-457.
- Chen, C.H., Cordova, P., Lai, W.C., Deierlein, G.G. and Tsai, K.C. (2004), "Pseudo-dynamic test of full-scale RCS frame. I: Design, construction and testing", *Proceedings of the 13th World Conference on Earthquake Engineering*, Vancouver, Canada, August.
- Chou, C.C. and Chen, J.H. (2010), "Tests and analyses of a full-scale post-tensioned RCS frame subassembly", *J. Construct. Steel Res.*, **66**(11), 1354-1365.
- Chou, C.C. and Wu, C.C. (2007), "Performance evaluation of steel reduced flange plate moment connections", *Earthq. Eng. Struct. Dyn.*, **36**(14), 2083-2097.
- Chou, C.C., Wang, C.Y. and Chen, J.H. (2008), "Seismic design and behavior of post-tensioned connections including effects of a composite slab", *Eng. Struct.*, **30**(11), 3014-3023.
- Cordova, P., Lai, W.C., Chen, C.H. and Tsai, K.C. (2004), "Pseudo-dynamic test of full-scale RCS frame. II:

- analyses and design implication”, *Proceedings of the 13th World Conference on Earthquake Engineering*, Vancouver, Canada, August.
- Fargier-Gabaldón, L.B. and Parra-Montesinos, G.J. (2006), “Behavior of reinforced concrete column-steel beam roof level T-connections under displacement reversals”, *J. Struct. Eng., ASCE*, **132**(7), 1041-1051.
- Guo, Z.X., Zhu, Q.Y. and Liu, Y. (2012), “Experimental study on seismic behaviors of a new type of prefabricated RCS frame connections”, *J. Build. Struct.*, **33**(7), 98-105. [In Chinese]
- Griffis, L.G. (1986), “Some design considerations for composite-frame structures”, *Eng. J.*, AISC Second Quarter, 59-64.
- Liang, X.M. and Parra-Moniesinos, G.J. (2004), “Seismic behavior of reinforced concrete column-steel beam subassemblies and frame systems”, *J. Struct. Eng., ASCE*, **130**(2), 310-319.
- Men, J.J. and Shi, Q.X. (2013), “ISCS method for the performance-based seismic design of vertically irregular RC frame structures”, *Struct. Des. Tall Special Build.*, **22**(11), 887-902.
- Men, J.J., Guo, Z.F. and Shi, Q.X. (2012), “Research on behavior of composite joints consisting of concrete and steel”, *Appl. Mech. Mater.*, **166-169**, 815-818.
- Michael, N.B., Joseph, M.B. and Walter, P.M.J. (2000), “Seismic behavior of composite RCS frame systems”, *J. Struct. Eng., ASCE*, **126**(4), 429-436.
- MOHURD (China Ministry of Housing and Urban-Rural Development) (2011), *Code for Seismic Design of Buildings* (GB 50011-2010); China Architecture & Building Press, Beijing, China. [In Chinese]
- Nozomu, B. and Yasushi, N. (2000), “Seismic behavior of RC column-s beam moment frames”, *Proceedings of the 12th World Conference on Earthquake Engineering*, Auckland, New Zealand, January-February.
- Parra-Montesions, G.J. and Weight, J.K. (2000), “Seismic response of exterior RC columns-to-steel beam connections”, *J. Struct. Eng., ASCE*, **126**(10), 1113-1121.
- SEOAC (Structural Engineering Association of California) (1995), *Vision 2000: Performance based seismic engineering of buildings*, California Office of Emergency Services; Vision 2000 Committee, CA, USA.
- Sheikh, T.M., Deierlein, G.G., Yura, J.A. and Jirsa, J.O. (1989), “Beam-column moment connections for composite frames: Part 1”, *J. Struct. Eng., ASCE*, **115**(11), 2858-2876.
- Wijesundara, K.K., Nascimbene, R. and Sullivan, T.J. (2011), “Equivalent viscous damping for steel concentrically braced frame structures”, *Bull Earthq. Eng.*, **9**(5), 1535-1558.

BU